

8-7-2019

The role of a permeable sand column in modifying tidal creek geochemistry and land-derived inputs to the coastal ocean

Nicholas Anthony Legut
Coastal Carolina University

Follow this and additional works at: <https://digitalcommons.coastal.edu/etd>



Part of the [Biogeochemistry Commons](#), [Geology Commons](#), and the [Oceanography Commons](#)

Recommended Citation

Legut, Nicholas Anthony, "The role of a permeable sand column in modifying tidal creek geochemistry and land-derived inputs to the coastal ocean" (2019). *Electronic Theses and Dissertations*. 112.
<https://digitalcommons.coastal.edu/etd/112>

This Thesis is brought to you for free and open access by the College of Graduate Studies and Research at CCU Digital Commons. It has been accepted for inclusion in Electronic Theses and Dissertations by an authorized administrator of CCU Digital Commons. For more information, please contact commons@coastal.edu.

**The role of a permeable sand column in modifying
tidal creek geochemistry and land-derived inputs to
the coastal ocean**

By
Nicholas A. Legut

Submitted in Partial Fulfillment of the Requirements for the Degree of Master of Science
In Coastal Marine and Wetland Studies in the School of the Coastal Environment
Coastal Carolina University
2019

Dr. Angelos Hannides, Major Professor

Dr. Erin Hackett, Committee Member

Dr. Richard Peterson, Committee Member

Dr. Rich Viso, Committee Member
and CMSS Department Chair

Dr. Michael Roberts, Dean,
College of Science

© Copyright 2019, Nicholas Anthony Legut (Coastal Carolina University)
All rights reserved. No part of this document may be reproduced or transmitted in any form or by any means, electronic, mechanical, photocopying, recording, or otherwise, without prior written permission of Nicholas Anthony Legut (Coastal Carolina University).

Dedication

I would like to dedicate this work to my family, friends, and my mentor, Dr. Angelos Hannides, who have all been instrumental in supporting and guiding me through the last two years. With you, I was able to make my dreams become reality. Thank you all.

Acknowledgements

Foremost, I would like to acknowledge Dr. Angelos Hannides giving me the opportunity to pursue higher education as your graduate student. I am honored to have worked under you. Kaitlin Dick, as a friend, and colleague, we have shared the majority of our graduate careers together. I could not thank you more for your support in the field and outside the field. I would like to acknowledge the following past and present students of the Sand Biogeochemistry Lab who have gone out of their way to help me: Ashaar Arbali, Lexi Echols, Rachel Birsch, Nick Workman, Brandon Hawkins, Desirae Vess, and Adam Hitt. These students have assisted on field sampling, methodology, or simply have been present to talk. I wish you all best of luck in your careers.

Again, thank you.

Abstract

The impairment of regional water quality in Long Bay is an episodic occurrence that has been documented for over a decade. According to one explanation, the occurrence of these events is hypothesized to be the combination of local, terrestrially derived inputs and water-column stratification in the nearshore zone. A portion of these inputs may discharge as surface run-off through estuaries ending in sandy transitional environments termed “swashes”. An investigation into the fate of land-derived materials through swashes utilize a linear conservative mixing model to describe the non-conservative behavior of materials in the overlying water and pore-water. This model relies on two endmembers to form a conservative mixing line across an environmental gradient along a transect located within the primary channel of the swash. Measured concentrations are plotted against the conservative mixing line to assess the chemical changes in properties which either result in the generation or removal of these properties with respect to the transect. The non-conservative behavior of these properties forms the basis for assessment on the role of a permeable sand column in modifying land-derived inputs. Highly permeable sediments ($2.9 \pm 1.1 \times 10^{-11} \text{ m}^2$) compose the sandy transect with which visually observed tidally-driven currents interact. Higher pore-water nutrient concentrations (dissolved inorganic nitrogen = 3-30 $\mu\text{mol/L}$) compared to overlying-water concentrations (3-30 $\mu\text{mol/L}$ vs. 0-20 $\mu\text{mol/L}$, respectively, for dissolved inorganic nitrogen) support the assumption that organic matter, filtered by the sandy sediment of the primary channel, is respired and nutrients are generated. Sedimentary chlorophyll concentrations are at least ten times as high as overlying-water chlorophyll

concentrations ($0\text{--}3\ \mu\text{g}/\text{cm}^3$ vs. $0\text{--}0.02\ \mu\text{g}/\text{cm}^3$, respectively), consistent with a “benthic nutrient filter”, whereby microphytobenthos are intercepting pore-water nutrients that are being transported upwards towards the overlying water. During periods of expected high primary productivity, the swash is a source of overlying-water oxygen and chlorophyll *a*, while at periods of expected low productivity, the swash is a source for nutrients and a sink for chlorophyll *a*. This transect study of the shoreline segment of Singleton Swash documents the role of a permeable sand column functioning as a biofilter. Inputs of nutrients from surface run-off ($35\ \mu\text{mol}/\text{L}$ and $4\ \mu\text{mol}/\text{L}$ for dissolved inorganic nitrogen and dissolved phosphate, respectively) resulted in high sedimentary chlorophyll concentrations but also a sink in both sedimentary chlorophyll and overlying-water oxygen, as expected in eutrophic conditions. These findings imply that the presence of a highly permeable sand column may be serving as an effective mitigation strategy for land-derived inputs of nutrients prior to reaching the coastal ocean, and must be given consideration in coastal engineering designs.

Table of contents

1	INTRODUCTION	1
1.1	Land-derived inputs to the coastal ocean.....	1
1.2	Swashes in the Grand Strand, South Carolina (SC).....	2
1.3	Key processes in sandy sediments of swashes.....	5
1.3.1	Physical exchange	5
1.3.2	Chemical transformations	6
1.3.3	Transformations along a freshwater-seawater transition	7
1.4	Study objectives	8
2	METHODS	9
2.1	Study area.....	9
2.2	Field observations and sampling.....	11
2.3	Analytical methods	12
2.4	Conservative mixing analysis	13
2.5	Statistical analysis	14
3	RESULTS	15
3.1	Meteorological and coastal oceanic conditions	15
3.2	Sedimentary geological and physical properties.....	15
3.3	Swash primary channel	19
3.3.1	Non-conservative behavior	23
3.3.2	Sediment-water column comparison.....	25
3.4	Comparisons with auxiliary stations	28
4	DISCUSSION	31
4.1	Sedimentary environment and physical exchange	31
4.2	Biogeochemistry of the primary channel	32
4.2.1	Spatial and temporal patterns	32
4.2.2	Non-conservative behavior	33
4.3	Human activities and their effects.....	34
4.3.1	Run-off from the surrounding area	34
4.3.2	Channel management.....	35
5	CONCLUSIONS.....	37
6	REFERENCES	38

Table of figures

Figure 1. Singleton Swash shown in three key phases. a) Extreme southward migration, b) beach nourishment and stabilization activities, c) post-nourishment and realignment. d) Hard seawall constructed as a last measure of protection for the Dunes Golf Clubhouse. e) Cross-sectional schematic of the proposed concrete culvert (USACE and DHEC, 2014). f) Aerial schematic of the proposed culvert (USACE and DHEC, 2014).	4
Figure 2. Diagram of non-conservative mixing adapted from Berner and Berner (1987).	8
Figure 3. Study site with approximate locations of primary channel and auxiliary stations (marsh tidal creek, sandy tidal pool, and run-off). Stations were spaced approximately 50 m apart between the yellow and red stars. A channel realignment took place on December 24 th , 2018.	10
Figure 4. Above: Atmospheric temperature and precipitation for North Myrtle Beach, the nearest National Weather Service station (NWS, 2019) and daylight duration estimated from sunrise and sunset times from the US Navy Observatory (USNO, 2019). Below: Coastal oceanic data collected from the Apache Pier station (4 m depth) of the Environmental Quality Laboratory of CCU (SECOORA, 2019). Sampling event times are shown in black circles and the time of Hurricane Florence is shown by the white triangle.	16
Figure 5. Sediment permeability along the transect. Distance of 0 m indicates the beginning of the transects (landward-most station; Figure 3).	17

Figure 6. Salinity and temperature variation with distance along the transect on all sampling dates. Distance of 0 m indicates the beginning of the transects (landward-most station; Figure 3).	18
Figure 7. Conservative mixing plots of overlying water biogeochemical properties. Solid black lines indicate conservative mixing lines. Error bars indicate one standard deviation where available.	20
Figure 8. Conservative mixing plots of sedimentary biogeochemical properties. Solid black lines indicate conservative mixing lines. Error bars indicate one standard deviation where available.	21
Figure 9. Box plots of concentrations of O ₂ (overlying water only), Chl <i>a</i> , DIN and PO ₄ ³⁻ along the transect (pore-water nutrient data not available on 12/12/2017). Mean values are indicated by the x.	22
Figure 10. Residuals for O ₂ (ΔO ₂ , overlying water only), Chl <i>a</i> (ΔChl <i>a</i>), DIN (ΔDIN) and phosphate (ΔPO ₄ ³⁻) in the primary swash channel on all main sampling dates. Positive residuals indicate net source, while negative residuals indicate a net sink. ..	24
Figure 11. Sedimentary (pore-water where “PW” is indicated) vs. overlying water (OW) concentrations for Chl <i>a</i> , DIN and PO ₄ ³⁻ for all stations along the transect on the main sampling dates. Dashed lines are ratios shown for ease of comparison.	26
Figure 12. The left column shows Sed Chl <i>a</i> vs overlying water (OW) % O ₂ saturation, DIN and PO ₄ ³⁻ at all sampling stations along the transect on the four main sampling dates and one preliminary sampling date (12/12/2017). The right column shows the average value for each sampling date along the transect.	27

Figure 13. Sedimentary geological and physical properties (mean \pm 1 standard deviation) of the primary swash channel, the sandy tidal pool and the marsh tidal channel across all sampling events.....	28
Figure 14. Segment of primary channel transect, adjacent to private property lawns behind metal wall (top), characterized by surface run-off (bottom) in January and April, 2019 (Photos courtesy of A. Hannides, April 14, 2019).	29
Figure 15. Mean (\pm 1 standard deviation) concentrations of O ₂ (overlying water only), Chl <i>a</i> , DIN and PO ₄ ³⁻ in the primary swash channel, the sandy tidal pool and the marsh tidal channel across all sampling events. Also shown are values for surface run-off in the overlying water plots.	30

List of symbols and/or abbreviations

%	Percent
b_{Model}	Modeled y-intercept
C_{Meas}	Measured concentration
C_{Model}	Modeled concentration
Chl <i>a</i>	Chlorophyll <i>a</i>
cm	Centimeter
DHEC	Department of Health and Environmental Control
DIN	Dissolved inorganic nitrogen
Eq	Equation
g	Gram
GF/F	Glass fiber filter
HDPE	High density polyethylene
L	Liter
LBOS	Long Bay Observation System
m	Meter
m_{Model}	Modeled slope
mL	Milliliter
mm	Millimeter
NWS	National Weather Service
O ₂	Oxygen
OW	Overlying water

p	p-value
Pa	Pascals
PO ₄ ³⁻	Phosphate
PW	Pore-water
Sal _{Meas}	Measured salinity
SC	South Carolina
SECOORA	Southeast Coastal Ocean Observing Regional Association
Sed	Sedimentary
SK ₁	Skewness
SWI	Sediment-water interface
USACE	United States Army Corps of Engineers
YSI	Yellow Springs Incorporated
ΔC	Residual of property C
μg	Microgram
μm	Micrometer
μmol L ⁻¹	Micromole per liter
σ ₁	Sorting

1 INTRODUCTION

1.1 Land-derived inputs to the coastal ocean

Populations in coastal regions of the US are continuously expanding at a rate of almost 10 % every ten years (NOAA, 2013). As land-use changes to accommodate growth, the increase in impervious surfaces results in a more rapid delivery of pollutants into water bodies and a decrease of freshwater infiltration into groundwater (Arnold and Gibbons, 1996). In shallow marine environments, excess nutrient input can result in the eutrophication of the water column and in severe cases, hypoxic conditions may develop (Howarth et al., 2011). These anthropogenic stressors alter the relative abundance of specific taxa and are strongly related to the degree of sediment contamination (Holland et al., 2004). It is therefore important to understand the processes that affect the magnitude of nutrient loading into coastal regions, specifically, natural features (estuaries and tidal creeks) that may mitigate the amount of nutrients entering the coastal ocean (Hedges and Kiel, 1995).

The impact of terrestrial systems on the coastal ocean is an interdisciplinary and a well-studied topic due to the direct effects of discharged materials. In Long Bay, South Carolina, episodic hypoxia has been investigated in multiple studies to describe the origin of these low-oxygen events. Two different explanations have been proposed for these hypoxic phenomena: 1) Discharge of highly saline, anoxic pore-water from offshore carbonate aquifers and advection of this water mass onshore by favorable winds (Peterson et al., 2016); 2) A combination of local, terrestrially derived inputs constrained

to the nearshore marine environment by a lack of mixing in the semi-enclosed Long Bay result in a drop in oxygen concentrations to hypoxic levels (Sanger et al., 2012; Troup et al., 2017). The latter theory suggests that tidal creeks and inlets play a large role in the delivery of matter to the nearshore zone. These transitional environments modify materials as they are transported into the coastal ocean and have a considerable effect on benthic and coastal ecology (Hedges and Kiel, 1995; Huettel et al., 2014). Understanding the role of sedimentary processes in mitigating anthropogenic loading to the coastal ocean will help guide future policies needed to sustain healthy coastal ecosystems.

1.2 Swashes in the Grand Strand, South Carolina (SC)

Estuarine tidal creeks are one of many conduits for freshwater run-off into the coastal ocean and represent the continuum from estuary to coastal marine environments (Smith and Sanger, 2015). The Grand Strand of SC spans approximately 100 kilometers (km) of high-energy sandy beaches (Barnhardt et al., 2009). Tidal creeks in the Grand Strand of South Carolina end at these broad sandy beaches and their flows, subjected to nearshore sediment transport processes, form transient meandering features termed “swashes” (Barnhardt et al., 2009). An extensive investigation of tidal creeks (ending in swashes) by Smith and Sanger (2015) concluded that a portion of land-derived materials were retained in their respective watershed prior to arrival to the swashes and discharge into the coastal ocean. The biogeochemical functions of the sandy swashes of estuarine tidal creeks are not fully understood, however they may contribute to episodic hypoxia in Long Bay (Sanger et al., 2012; Smith and Sanger, 2015).

Many sandy beaches in the region are susceptible to erosion, exacerbated by sea level rise (Barnhardt et al., 2009). Migrating swashes may amplify the problem by threatening to erode private property as well as preventing flushing of estuaries (Hoffnagle, 2015). “Soft” remediation efforts may include realignment of the tidal channels and reconstruction of beach profiles during renourishment, while “hard” armored protection involves building solid-bottom culverts that would stabilize the tidal channel, or constructing seawalls (USACE and DHEC, 2018). Examples of the above are shown in Figure 1 for Singleton Swash, SC. Impervious culverts would prevent natural biogeochemical transformations from occurring in the sandy sediment column and thus would increase the discharge of dissolved and particulate constituents into the coastal ocean. The environmental effect from these engineering solutions may be overlooked in sandy intertidal regions, where the critical living communities are often burrowing (infauna), microscopic, or transient, and therefore not immediately evident to the naked eye (Speybroeck et al., 2006). Consideration must be given to these intertidal communities, as they facilitate the earliest transformations of land-derived inputs carried to the coastal ocean.

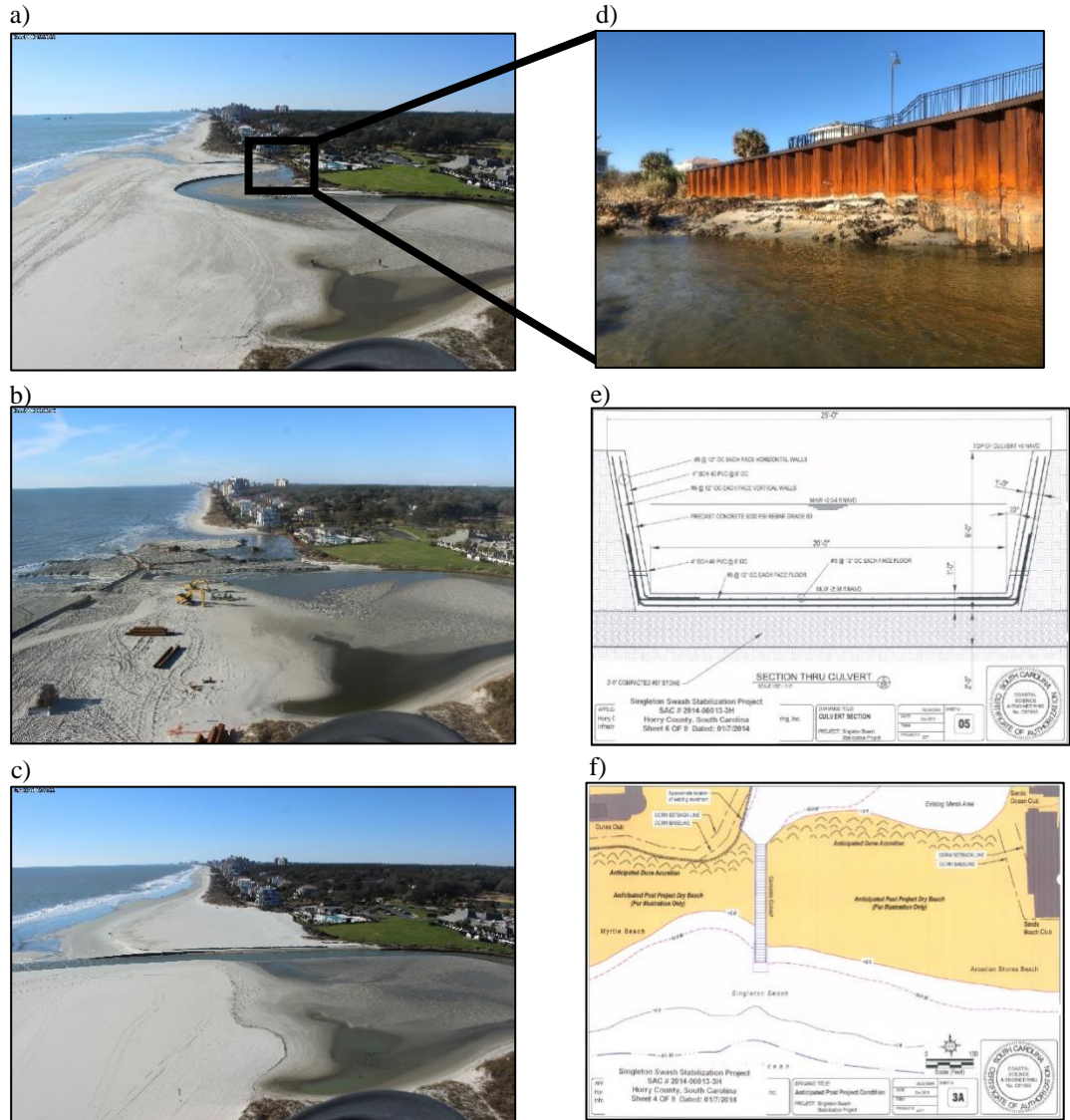


Figure 1. Singleton Swash shown in three key phases. a) Extreme southward migration, b) beach nourishment and stabilization activities, c) post-nourishment and realignment. d) Hard seawall constructed as a last measure of protection for the Dunes Golf Clubhouse. e) Cross-sectional schematic of the proposed concrete culvert (USACE and DHEC, 2014). f) Aerial schematic of the proposed culvert (USACE and DHEC, 2014).

1.3 Key processes in sandy sediments of swashes

1.3.1 Physical exchange

Swashes are primarily sandy environments and are heavily influenced by nearshore processes. The physical reworking of sediments causes fine grain sediments to be transported away from the site of high energy (swashes), resulting in a highly permeable sandy environment (Hjulestrom, 1939; Boudreau et al., 2001). Another key feature in energetic sandy environments is bathymetry. In addition to burrows and debris, flows over non-cohesive sandy sediments will generate ripples, which contribute to the bathymetry of this setting (Allen, 1968).

When the aforementioned setting is present, bottom boundary layer flows and sediment bathymetry result in significant interactions between sand and the overlying water column (Huettel et al., 1996). These interactions are characterized by turbulent, advection-driven flows, which induce vertical transport across the sediment-water interface (SWI; Berg et al., 2003; Chipman et al., 2016). These flows over sediment bathymetry induce pressure gradient forces, driving overlying water into the sediment upstream of bathymetric features and upwelling pore-water downstream of these features (Huettel et al., 1996; Elliot and Brooks, 1997). Pressure gradients as small as 1 Pa/cm over small sediment ripples have been shown to force water several centimeters into the sediment and upwell pore-water from as deep as 10 centimeters into the water column (Huettel and Gust, 1992). This physical exchange transports matter, both particulate and dissolved, through permeable sediments at orders-of-magnitude higher rates than

gravitational settling and molecular diffusion and may be an effective mixing process between the overlying water and pore-water of permeable sediments (Huettel et al., 1998; Precht and Huettel, 2004).

1.3.2 Chemical transformations

The rapid turnover of materials in permeable sand is reflected by low organic carbon and nutrient concentrations in the overlying water and uppermost sediment layer (Webb and Theodor, 1968; Huettel et al., 1998). This exchange is coupled with benthic ecology and has been studied extensively over a variety of spatial and temporal scales (Boulton et al., 1998; Schutte et al., 2013; Chipman et al., 2016; Kim et al., 2017). In swashes, where physical transport is present, and the water column is shallow, transformations of organic materials by microbial respiration are likely to occur in the sediment rather than the water column (Berner, 1980). Sedimentary respiration (left-to-right direction in Eq. 1, based on Froelich et al., 1978, using Redfield-Richards stoichiometry) releases dissolved inorganic nutrients into the pore-water where they may be subject to physical transport:



Without any further transformations, these dissolved inorganic nutrients would be circulated back into the water column by advective pore-water flows (Webb and Theodor, 1968). However, a highly abundant biofilm of microphytobenthic communities, on the order of millions of cells per cubic centimeter, are able to photosynthesize in the top 5 millimeters (mm) of photic permeable sediment (MacIntyre et al., 1996). This biofilm may assimilate dissolved inorganic nutrients derived from the sedimentary

nutrient pool during photosynthesis (right-to-left direction in Eq. 1), acting as a living filter (Webb and Theodor, 1968; Savant et al., 1987). These benthic primary producers have been shown to behave analogous to their phytoplanktonic counterparts and with respect to sandy settings may be as abundant if not more abundant than phytoplankton (Pinckney et al., 1995).

1.3.3 Transformations along a freshwater-seawater transition

Chemical processes occurring in estuaries, where freshwater encounters and mixes with seawater, can be evaluated using the non-conservative mixing approach to describe the in-situ production or removal of a material by physical and chemical processes with respect to a conservative tracer such as salinity (Libes, 2009). Physical mixing between two distinct endmembers results in intermediate concentrations of a chemical, predicted by the chemical's concentration in the two endmembers and their volume mixing ratio at a specific location. In the case where physical mixing is the dominant process along this gradient, the intermediate concentrations fall on a straight line, representing conservative mixing. If measured concentrations lie above or below the conservative mixing line, the net outcome of all other processes affecting the chemical in this area is addition (production) or removal (consumption), respectively (Figure 2) (Berner and Berner, 1987). While this method has been extensively applied to large estuaries (Raymond et al., 2000), it may also be proven useful as an indicator of changes in both overlying-water and sedimentary concentrations in smaller features such as swashes.

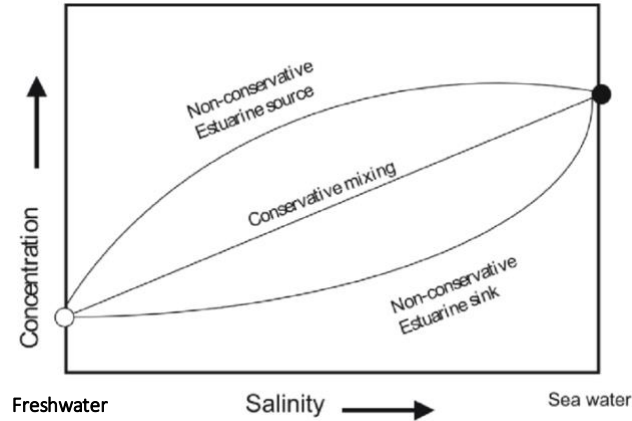


Figure 2. Diagram of non-conservative mixing adapted from Berner and Berner (1987).

1.4 Study objectives

Our study examines the role of a swash, the sandy transitional zone between a marsh and the coastal ocean, in biogeochemical transformations of land-derived inputs from a heavily modified urban watershed. A high-resolution transect was sampled throughout the swash's primary channel across five different sampling dates to identify changes in a suite of water-column and sedimentary parameters with particular attention to the function of the underlying permeable sand column. The chemical and biological change in concentrations of various dissolved nutrients and particulate materials in the overlying water and in the sediment along the transect is supplemented by assessing the non-conservative behavior of these nutrients and materials. In addition, the character of the above under seasonal variation in light and temperature is investigated. Our findings form the basis for understanding how sandy transitional settings mitigate the impact of terrestrially derived inputs on coastal-ocean water quality in a relatively under-studied environment.

2 METHODS

2.1 Study area

Singleton Swash, a heavily modified estuarine “swash” typical of others in the Grand Strand of South Carolina (Smith and Sanger, 2015) was selected as our study site due to the potential for biogeochemical transformations in a sandy setting. A primary tidal channel cuts through the sandy swash and meanders around a small sandy tidal flat which experiences semi-diurnal inundation by tides (Figure 3). The primary channel is influenced heavily by nearshore processes, which results in high sedimentation rates and a dynamic morphology (Hoffnagle, 2015).

Singleton Swash drains the third largest watershed (613 hectares) of 15 swashes identified by Smith and Sanger (2015). Pastore (2018) calculated discharge out of Singleton Swash to be $4.52 \times 10^5 \text{ m}^3$ per ebb tide. In addition, the impervious cover (percentage) of land around Singleton Swash is 20.1% (Smith and Sanger, 2015).

Sampling stations were selected for a high-resolution transect (50-m resolution) spanning from a relatively stable transition zone (Figure 3, indicated by star), through the swash zone. Auxiliary stations, e.g., in the mud-dominated marsh tidal creek segment and in a sandy tidal pool, were added as well to provide contrast against the sandy tidal creek transect (Figure 3). In addition, surface run-off (Figure 3) at the banks of the channel adjacent to a nearby property was also sampled when present.

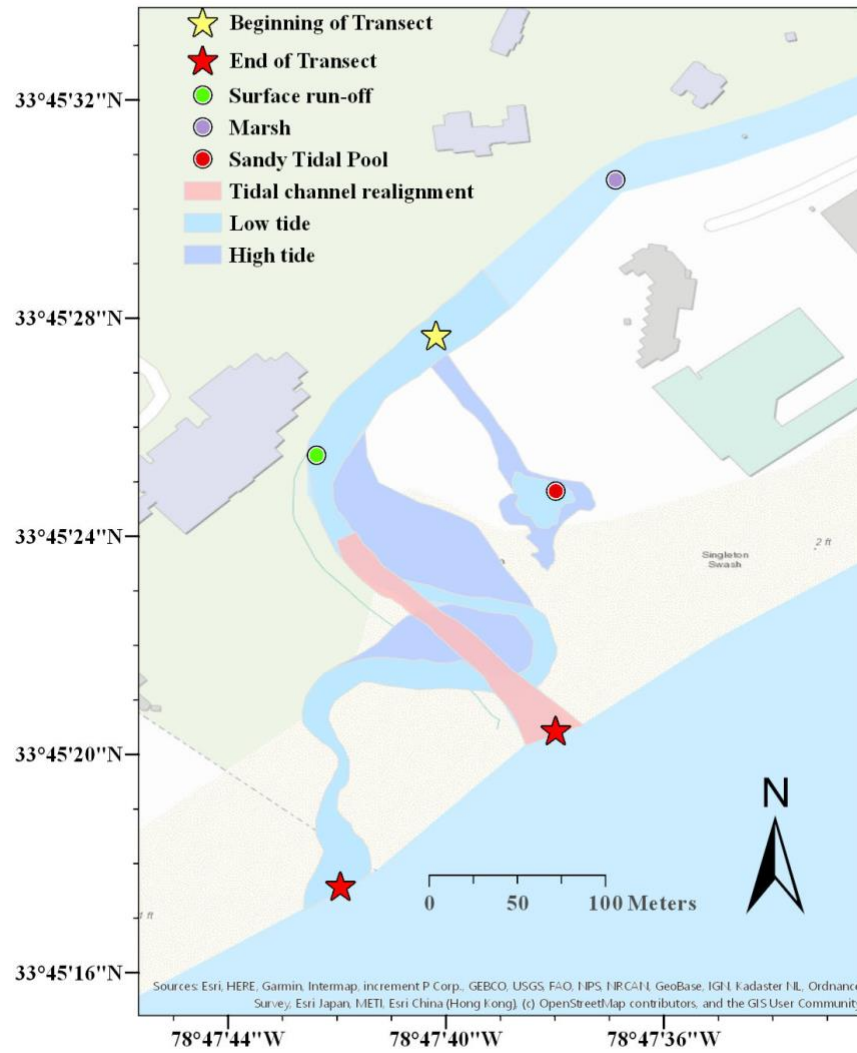


Figure 3. Study site with approximate locations of primary channel and auxiliary stations (marsh tidal creek, sandy tidal pool, and run-off). Stations were spaced approximately 50 m apart between the yellow and red stars. A channel realignment took place on December 24th, 2018.

2.2 Field observations and sampling

We chose to sample seasonally due to considerable variation in light and temperature during an annual cycle. Atmospheric data were collected from the national weather service to identify the ambient changes in abiotic factors and anomalies, if present (NWS, 2019). Water conditions (water temperature and salinity) in Long Bay, SC were obtained from the Long Bay Observation System at Apache Pier, SC, through the SECOORA data portal (LBOS, 2019). We expect that the dynamic conditions, and a shallow water column, cause changes in oxygen (O_2), chlorophyll *a* (Chl *a*), and inorganic nutrients as the balance between photosynthesis and respirations shifts. After conducting preliminary sampling on December 12th, 2017 and August 15th, 2018, seasonal sampling began on August 31st, 2018. Subsequent sampling events occurred on November 17th, 2018, January 22nd, 2019 and April 14th, 2019. Sampling events consisted of field measurements and laboratory analyses. Five to ten sampling locations were selected roughly every 50 m spanning the distance from the beach swash zone to the point the (spatially stable) tidal creek enters the sand field, representing a high-resolution transect across the primary tidal channel.

At every station, a YSI ProDSS meter (YSI Inc., Yellow Springs, Ohio) was used to record the station's GPS location, water temperature ($^{\circ}C$), salinity (PSU) and O_2 (% saturation), while turbidity (NTU) was measured using a HACH 2000Q portable turbidimeter (Hach, Loveland, Colorado). Water-column and sedimentary samples were retrieved from the same locations. Water samples were filtered on site through 0.2- μm nylon filters into 7-mL, pre-rinsed scintillation vials for inorganic nutrient analyses.

Additional water samples were collected in 125-mL HDPE bottles for filtering on GF/F filters in the lab for Chl *a* analysis. Surface sediment (0-10 cm) samples for laboratory analysis of grain-size distribution and permeability were collected using 60-mL cut-off syringes, and sedimentary (Sed) Chl *a* samples (0-5 cm) were collected using 10-mL cut-off syringes and transferred to pre-weighed glass vials. Pore-water samples were retrieved using an MHE PushPoint sampler (MHE Products, East Tawas, Michigan) at 30 cm below the sediment surface. All samples were immediately stored on ice in a cooler, transported to the lab within an hour, and stored in the freezer or processed immediately.

2.3 Analytical methods

Permeability was determined by the constant-head method (Klute and Dirksen, 1986; Rocha et al., 2005). Grain size distribution was determined by wet sieving and mean grain size (mm, phi), median grain size (mm, phi), sorting (phi), and skewness (dimensionless) were determined by the statistical definitions in McManus (1988).

Chl *a* was measured by fluorescence after extraction in acetone as described for GF/F filters in Arar and Collins (1999) and for sedimentary samples in Hannides et al. (2014).

The methods used for nutrient analyses in this study have been modified to accommodate small sample volumes (1-1.2 ml) in order to minimize the volume of the sampled effective sediment sphere. A microvolume column was set up for the reduction of nitrate (NO_3^-) to nitrite (NO_2^-), according to the principles in Strickland and Parsons (1972), and nitrite was analyzed spectrophotometrically (Bendschneider and Robinson, 1952), with limits of detection of 0.37 and 0.02 $\mu\text{mol L}^{-1}$ for nitrate and nitrite

respectively. Ammonium (NH_4^+) was analyzed by fluorescence according to Holmes et al. (1999), with a limit of detection of $0.17 \mu\text{mol L}^{-1}$. Phosphate (PO_4^{3-}) was analyzed spectrophotometrically by the molybdenum blue complexation method with a limit of detection at $0.26 \mu\text{mol L}^{-1}$ (Murphy and Riley, 1962; Hansen and Koroleff, 1999).

2.4 Conservative mixing analysis

Linear conservative mixing models (Figure 2) were developed by fitting a linear regression model through the two salinity end-member (x-axis) vs. chemical concentration (y-axis) pairs using MS Excel in the primary tidal channel on each sampling event, yielding a model slope (m_{Model}) and a model intercept (b_{Model}).

Deviation from conservative mixing, ΔC (otherwise known as the residual value), was quantified as follows:

$$\Delta C = C_{\text{Meas}} - C_{\text{Model}} \quad 2$$

where C can be replaced by the formula or notation of the compound under investigation, C_{Meas} is the measured concentration at non-end-member stations and C_{Model} is the theoretical concentration predicted by the linear conservative mixing model, as follows:

$$C_{\text{Model}} = m_{\text{Model}} \times \text{Sal}_{\text{Meas}} + b_{\text{Model}} \quad 3$$

where Sal_{Meas} is the measured salinity at a non-end-member station, m is the slope of the linear model and b is the intercept of the linear model.

The resulting residual values for any given property on any given sampling event were analyzed statistically to evaluate source/sink behavior and similarities between seasons and properties to determine the overall behavior of various chemicals in Singleton Swash.

2.5 Statistical analysis

Data were explored graphically and statistically using suitable methods (Sokal and Rohlf, 1994). Property-property plots, including the salinity vs. concentration plots used in the conservative mixing analysis, were generated using averages (and standard deviations) of each property at each station. Deviations from conservative behavior for each property were evaluated by constructing Box and Whisker plots (MS Excel) of residual values throughout the swash for each property on each sampling event. These plots displayed the 25-75 % range or interquartile range (box), the 1.5×interquartile range (whiskers), the median (line), and mean (indicated as “x”) along the transect. The assessment of non-conservative behavior for a measured property was determined by the position of the 25-75% interquartile range relative to zero. One-tailed ANOVA was used to determine if significant differences in the concentrations of O₂, nutrients and Chl *a* existed between seasons as well as between the sedimentary and overlying water environments (significance level of 0.01).

3 RESULTS

3.1 Meteorological and coastal oceanic conditions

Meteorological and coastal oceanic data are shown to provide information on abiotic factors during the study (Figure 4). Atmospheric temperature and daylight duration show typical seasonal variation increasing during the summer and decreasing during the winter, while precipitation records document intense rainfall events, especially Hurricane Florence (September 2018). The effect of this event is noticeable in coastal ocean data collected at the nearby Apache Pier station of the Environmental Quality Lab of CCU. While sea surface temperature displays regular seasonal variation, salinity is significantly lower immediately after Hurricane Florence and remains below normal oceanic salinity for the remainder of the study period.

3.2 Sedimentary geological and physical properties

Sedimentary and physical properties across the study site are summarized in Table 1. Overall the sediment along the primary channel may be classified as moderately sorted, medium sand, with a symmetrical distribution. Sediment is highly permeable ($>10^{-12} \text{ m}^2$) and decreases towards the landward-most station (Figure 5).

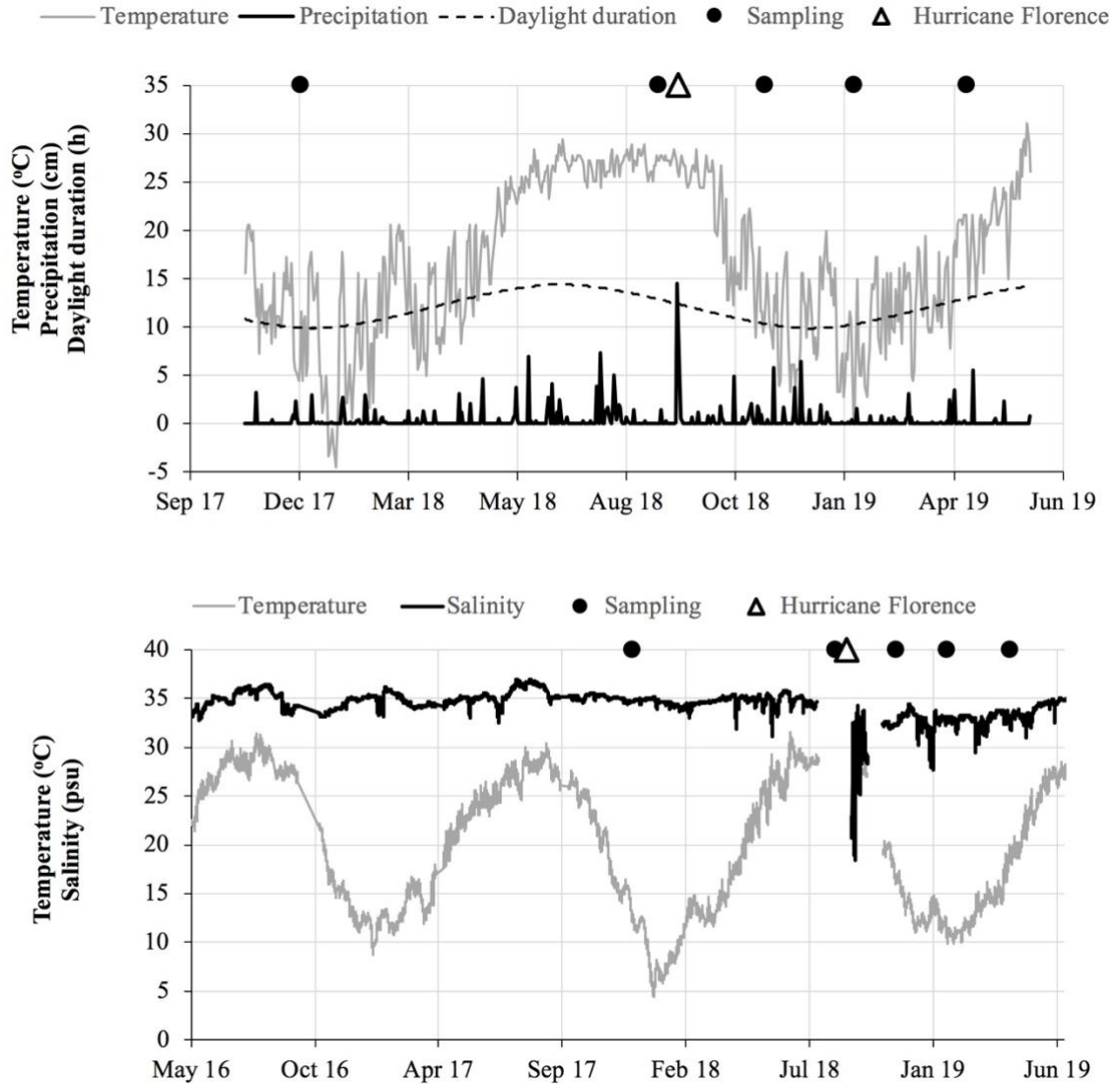


Figure 4. Above: Atmospheric temperature and precipitation for North Myrtle Beach, the nearest National Weather Service station (NWS, 2019) and daylight duration estimated from sunrise and sunset times from the US Navy Observatory (USNO, 2019). Below: Coastal oceanic data collected from the Apache Pier station (4 m depth) of the Environmental Quality Laboratory of CCU (SECOORA, 2019). Sampling event times are shown in black circles and the time of Hurricane Florence is shown by the white triangle.

Table 1. Sedimentary geological and physical properties (average \pm 1 standard deviation).

	Primary channel	Marsh tidal creek	Sandy tidal pool
Mean grain size (phi, μm)	1.87 ± 0.36 , 282 ± 62	2.5, 182	2.2 ± 0.2 , 220 ± 29
Median grain size (phi, μm)	1.87 ± 0.37 , 282 ± 60	2.6, 164	2.3 ± 0.3 , 210 ± 45
Sorting			
σ_1	0.72 ± 0.12	0.68 ± 0.34	0.76 ± 0.03
classification	Moderately sorted	Moderately well sorted	Moderately sorted
Skewness			
SK_1	-0.04 ± 0.12	-0.34	-0.13 ± 0.19
classification	Symmetrical	Very negatively skewed	Negatively skewed
Permeability (m^2)	$2.9 \times 10^{-11} \pm 1.1 \times 10^{-11}$	$1.4 \times 10^{-12} \pm 5.5 \times 10^{-13}$	$4.7 \times 10^{-12} \pm 3.0 \times 10^{-12}$
Porosity	0.44 ± 0.02	0.46 ± 0.01	0.45 ± 0.00

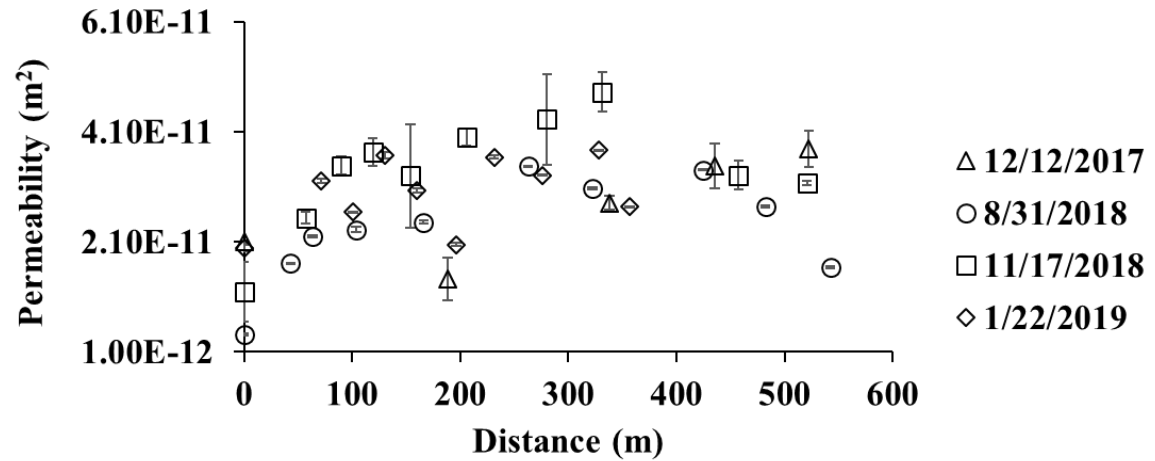


Figure 5. Sediment permeability along the transect. Distance of 0 m indicates the beginning of the transects (landward-most station; Figure 3).

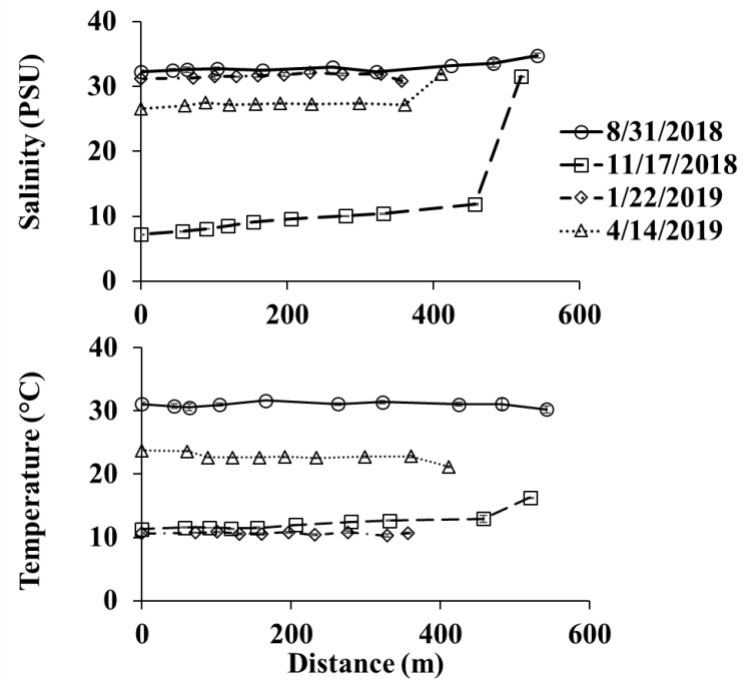


Figure 6. Salinity and temperature variation with distance along the transect on all sampling dates. Distance of 0 m indicates the beginning of the transects (landward-most station; Figure 3).

3.3 Swash primary channel

Salinity and temperature variations with distance in the primary channel on all dates are shown in Figure 6.

Biogeochemical data from the overlying water and sediment of the primary channel from the four main sampling events are shown as conservative mixing plots in Figure 7 and Figure 8, respectively, and as box plots in Figure 9. Statistically significant differences were detected between sampling events in all water-column properties during the study ($p < 1 \times 10^{-5}$) and Sed Chl *a* ($p = 4 \times 10^{-4}$), but no such differences were present in the remaining sedimentary properties ($p = 0.851$, PW DIN; $p = 0.151$, PW PO_4^{3-}).

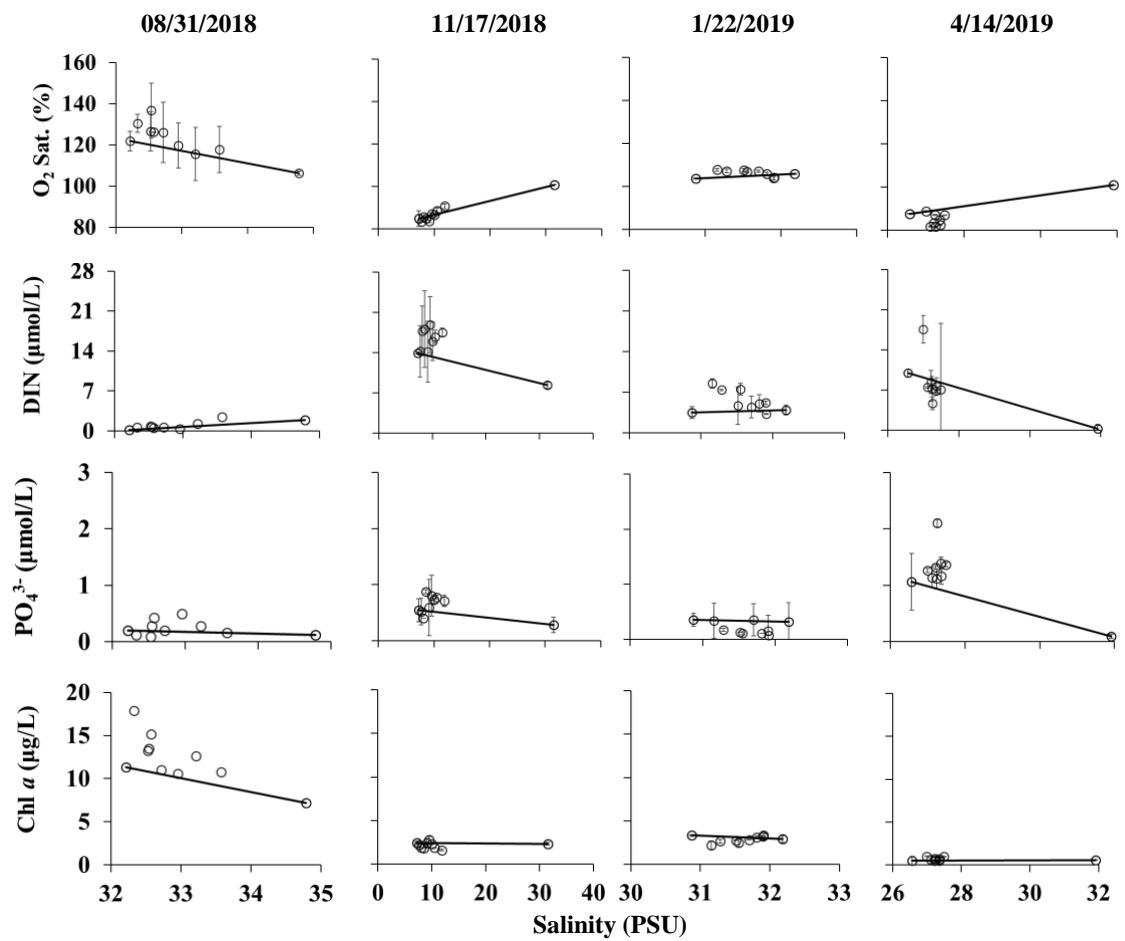


Figure 7. Conservative mixing plots of overlying water biogeochemical properties. Solid black lines indicate conservative mixing lines. Error bars indicate one standard deviation where available.

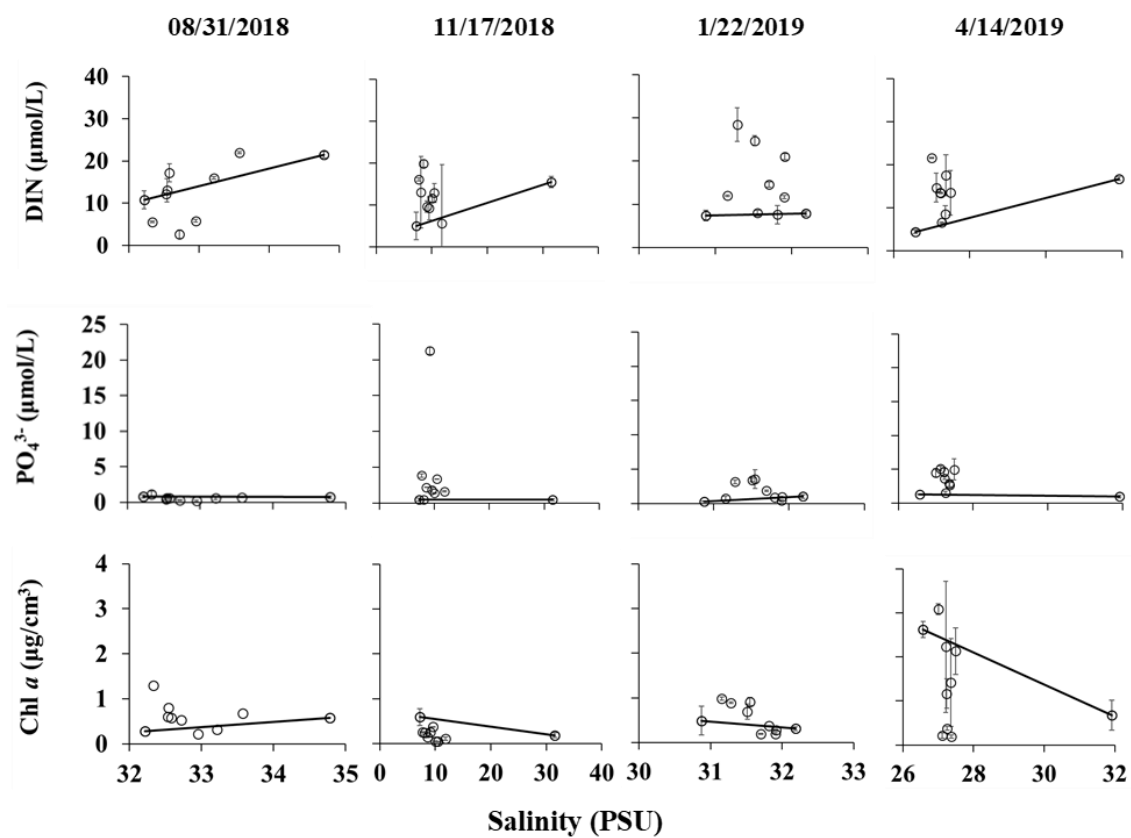


Figure 8. Conservative mixing plots of sedimentary biogeochemical properties. Solid black lines indicate conservative mixing lines. Error bars indicate one standard deviation where available.

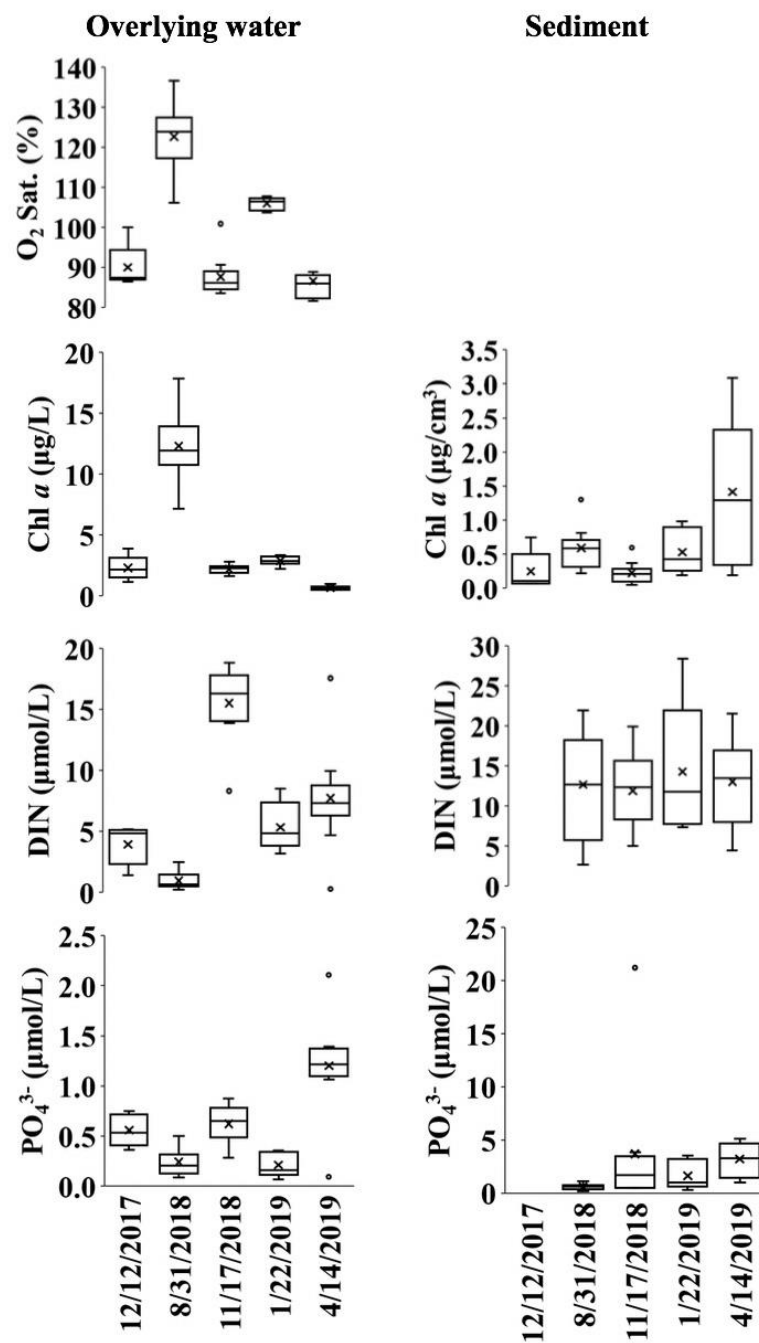


Figure 9. Box plots of concentrations of O₂ (overlying water only), Chl *a*, DIN and PO₄³⁻ along the transect (pore-water nutrient data not available on 12/12/2017). Mean values are indicated by the x.

3.3.1 Non-conservative behavior

Residuals calculated during the conservative mixing analysis are shown in Figure 10, and source/sink designation for each property on each day is summarized in Table 2.

Table 2. Source/sink behavior for measured overlying water (OW), pore-water (PW) and sedimentary (Sed) properties based on the position of the 25-75% interquartile range relative to zero. Dash indicates mixed behavior along the complete transect.

Date	8/31/2018	11/17/2018	1/22/2019	4/14/2019
% O ₂	Source	-	-	Sink
OW Chl <i>a</i>	Source	Sink	-	-
OW DIN	-	Source	Source	Sink
OW PO ₄ ³⁻	-	Source	Sink	Source
Sed Chl <i>a</i>	Source	Sink	Source	Sink
PW DIN	-	Source	Source	Source
PW PO ₄ ³⁻	Sink	Source	Source	Source

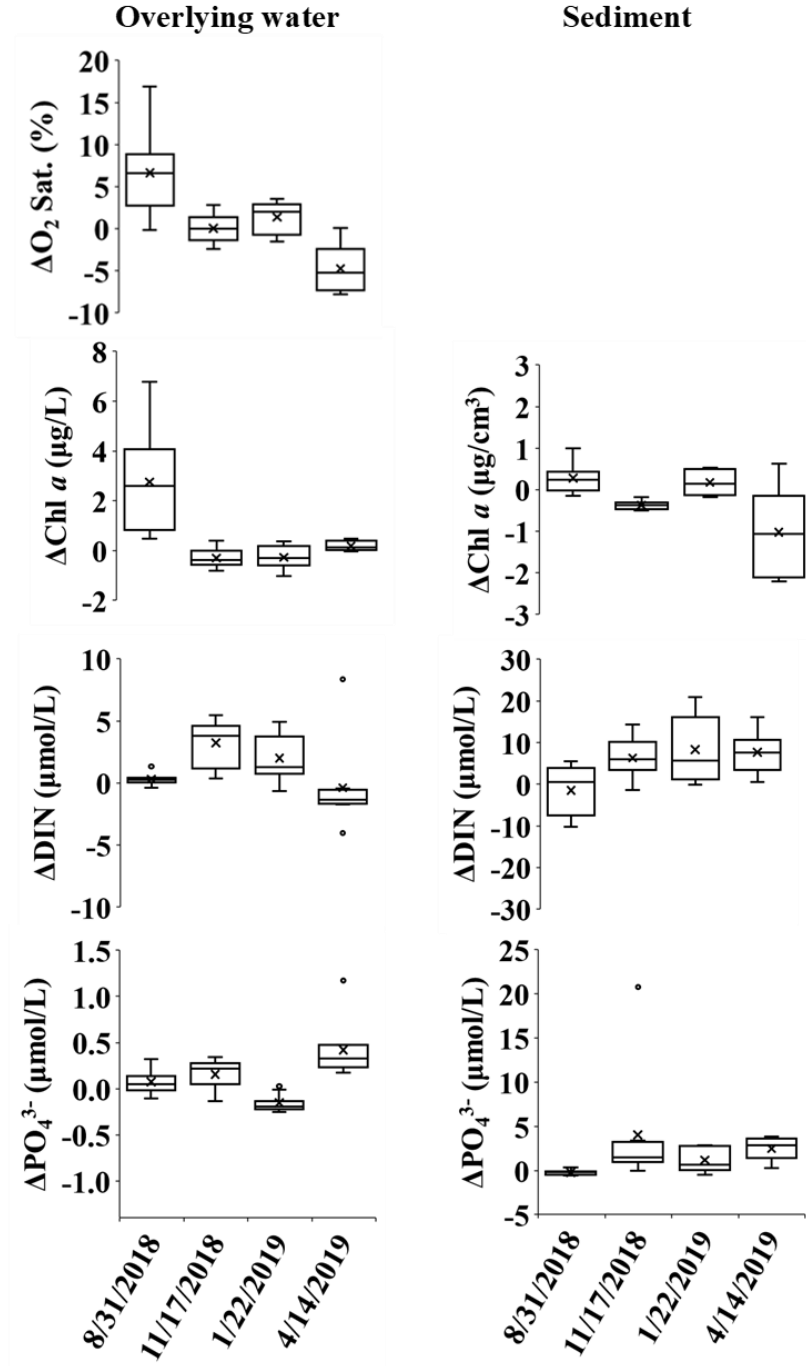


Figure 10. Residuals for O_2 (ΔO_2 , overlying water only), $\text{Chl } a$ ($\Delta \text{Chl } a$), DIN (ΔDIN) and phosphate (ΔPO_4^{3-}) in the primary swash channel on all main sampling dates. Positive residuals indicate net source, while negative residuals indicate a net sink.

3.3.2 Sediment-water column comparison

Sedimentary vs. overlying water concentrations of Chl *a*, DIN, and PO₄³⁻ in the primary swash channel on the main sampling dates are shown in Figure 11. Sedimentary concentrations are higher than overlying water concentrations ($p < 0.01$) on all occasions with the exception of inorganic nutrients on 11/17/2018 ($p = 0.056$, DIN; $p = 0.140$, PO₄³⁻) and DIN on 4/14/2019 ($p = 0.024$).

The relationship between Sed Chl *a* concentrations and overlying-water O₂ saturation, DIN and PO₄³⁻ concentrations at each station on the main sampling dates are shown in Figure 12.

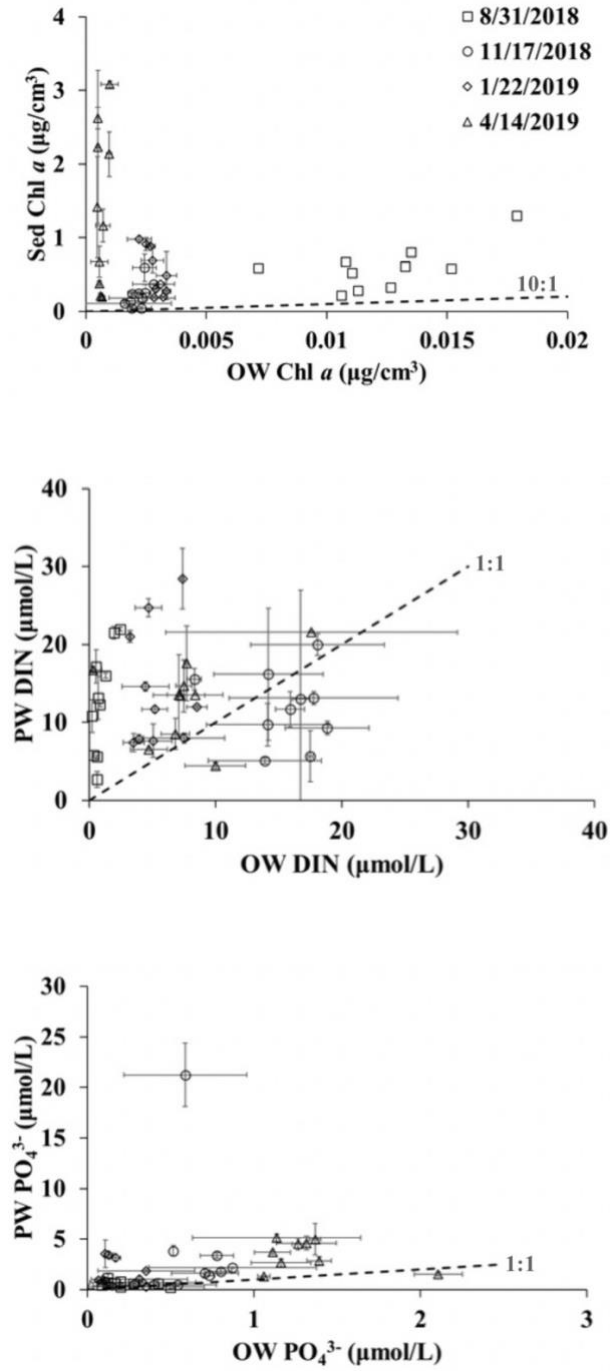


Figure 11. Sedimentary (pore-water where “PW” is indicated) vs. overlying water (OW) concentrations for Chl *a*, DIN and PO_4^{3-} for all stations along the transect on the main sampling dates. Dashed lines are ratios shown for ease of comparison.

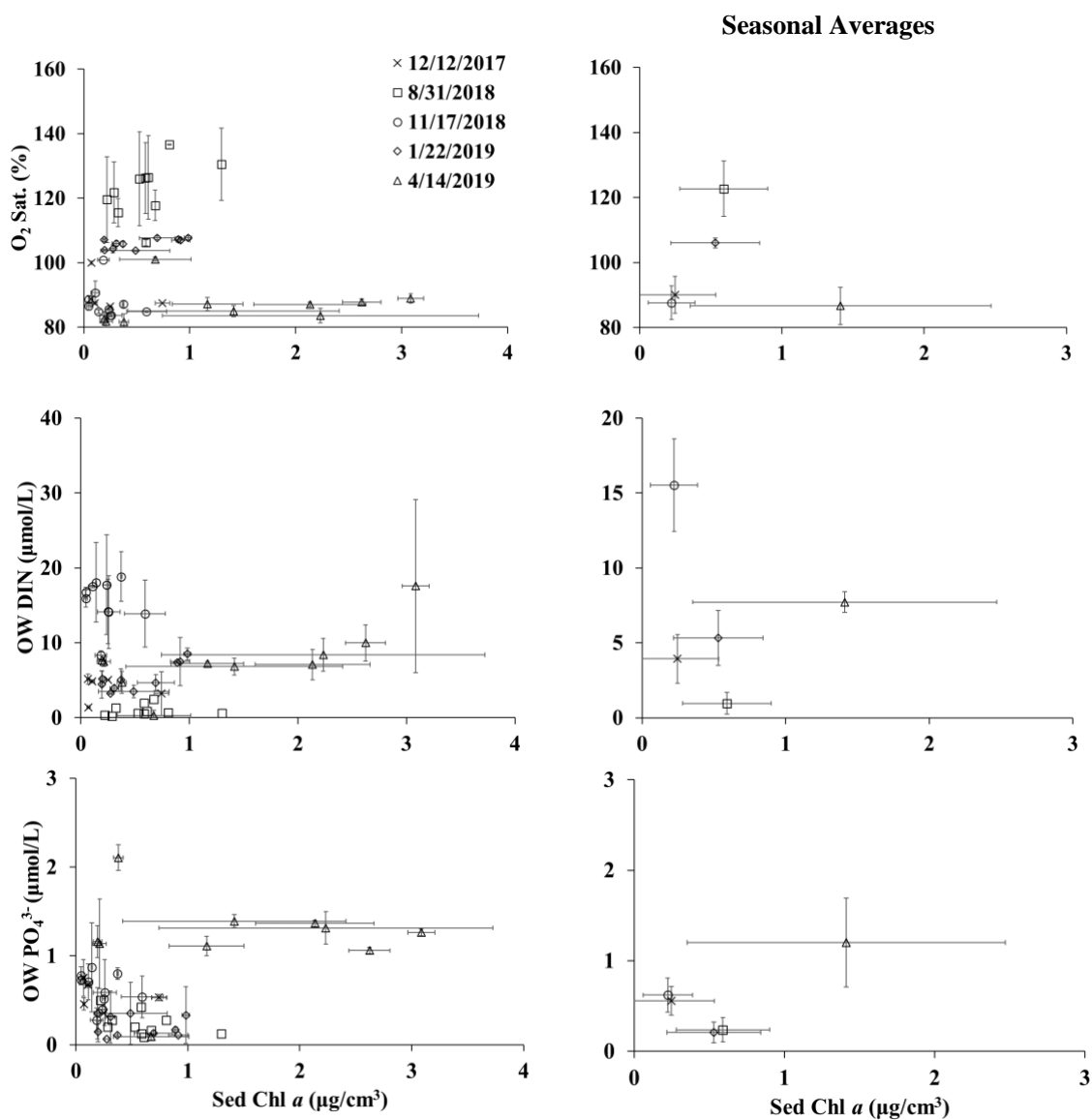


Figure 12. The left column shows Sed Chl *a* vs overlying water (OW) % O₂ saturation, DIN and PO₄³⁻ at all sampling stations along the transect on the four main sampling dates and one preliminary sampling date (12/12/2017). The right column shows the average value for each sampling date along the transect.

3.4 Comparisons with auxiliary stations

Auxiliary stations such as the marsh tidal channel and a sandy tidal pool flushed at high tide represent a contrast to the primary swash channel. Sedimentary physical and geological properties at the three stations and sampling events are compared in Figure 13.

In addition to these three sites, the occasional occurrence of considerable surface water run-off from the adjacent golf course into the primary swash channel, accompanied by substantial macroalgal growth on hard substrates on the banks (Figure 14) , during the January and April, 2019, sampling events warranted study, and therefore was included as an auxiliary station. A comparison of biogeochemical properties in both overlying water and sediment across all four stations is shown in Figure 15.

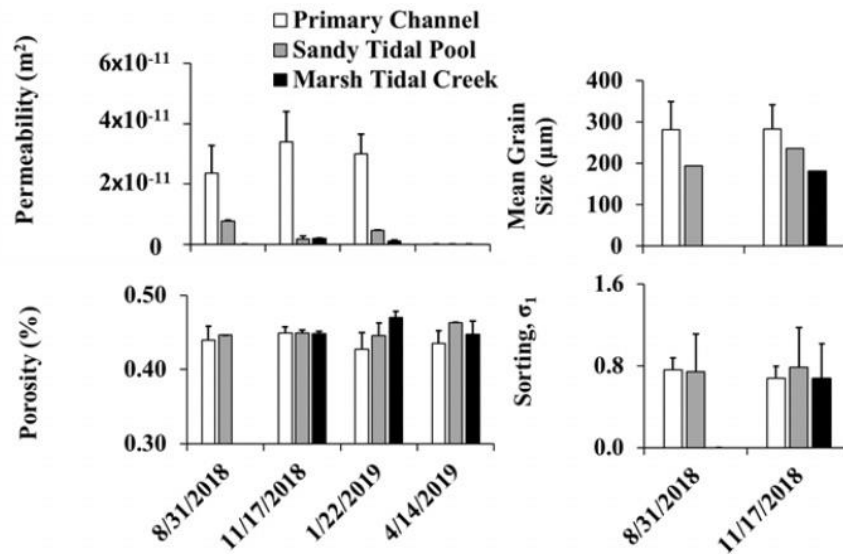


Figure 13. Sedimentary geological and physical properties (mean ± 1 standard deviation) of the primary swash channel, the sandy tidal pool and the marsh tidal channel across all sampling events.



Figure 14. Segment of primary channel transect, adjacent to private property lawns behind metal wall (top), characterized by surface run-off (bottom) in January and April, 2019 (Photos courtesy of A. Hannides, April 14, 2019).

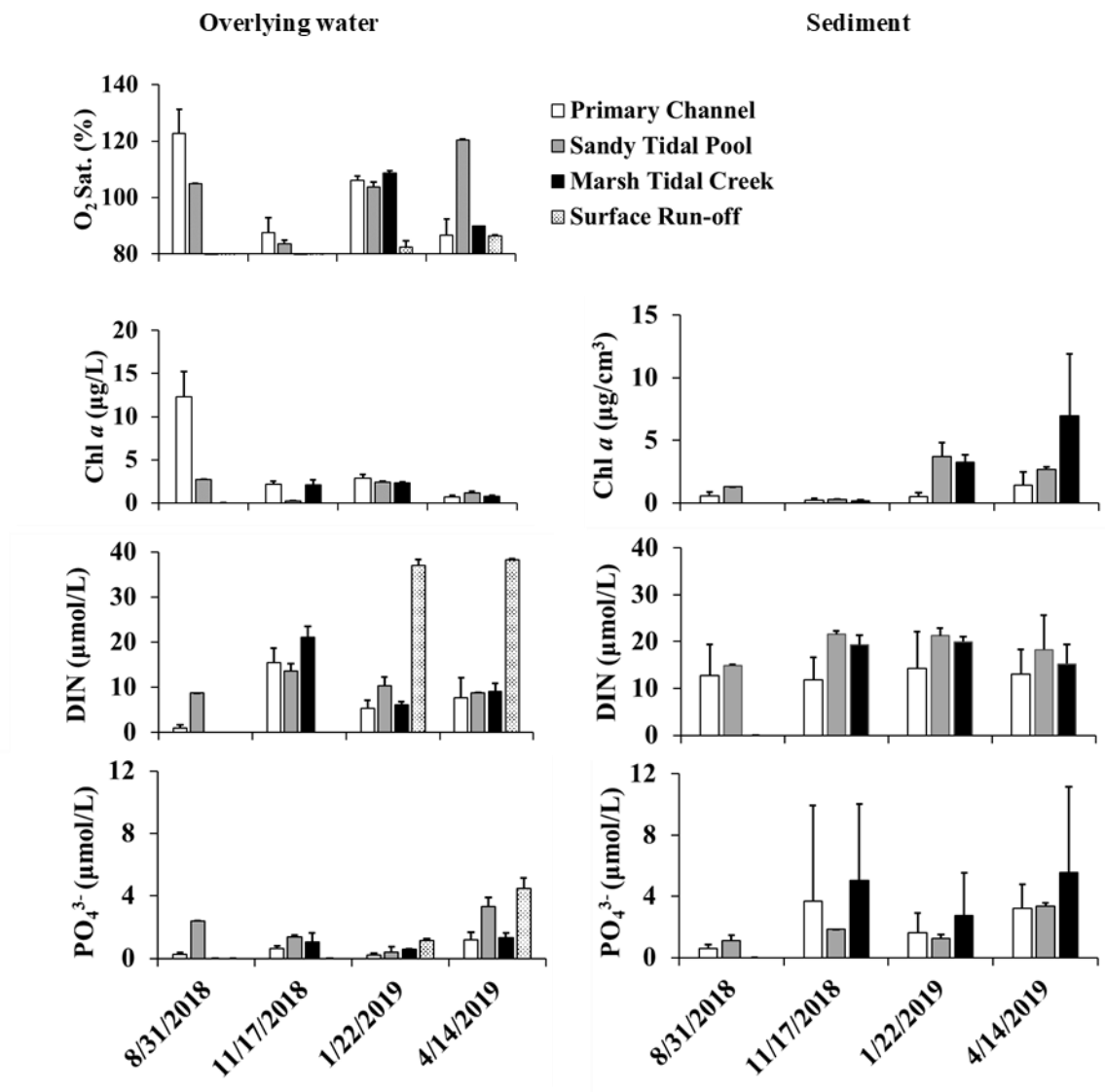


Figure 15. Mean (± 1 standard deviation) concentrations of O₂ (overlying water only), Chl *a*, DIN and PO₄³⁻ in the primary swash channel, the sandy tidal pool and the marsh tidal channel across all sampling events. Also shown are values for surface run-off in the overlying water plots.

4 DISCUSSION

4.1 Sedimentary environment and physical exchange

The primary channel of Singleton Swash is composed of highly permeable, medium sand (Figure 5). In contrast, sediment in the sandy tidal pool and marsh tidal creek consists of finer sand than the primary channel and, consequently, permeabilities that are lower by 6 and 20 times, respectively, due to larger fractions of fine-grained sediments (grain diameter $< 63 \mu\text{m}$) than primary channel sand (Figure 13).

While the direct exchange of matter across this highly permeable SWI was not measured, it is likely this exchange occurs at a greater rate along the transect than in less permeable environments (marsh tidal creek). Visually observed fast current speeds of overlying water combined with a highly permeable sedimentary column, likely result in exchange of particulate and dissolved materials across the SWI.

The rapid water currents and uneven bathymetry that were observed along the transect suggest the overlying water mixes rapidly in the primary channel via turbulent forces (Berg et al., 2003). Increased tidal exchange by channel realignment and rapid mixing reflect small variations in salinity and temperature within the primary swash channel, with the ocean end-member being more distinct than the rest of the swash samples (Figure 6). The uniformity in temperature and salinity is consistent with a water mass accumulating within the marsh tidal creek and emptying out during low tide (Pastore, 2018).

The lack of a gradual freshwater-seawater transition in the primary channel, as is typical of large estuaries, is accompanied by mid-transect salinity minima, e.g., on August, 2018, and April, 2019 (Figure 6). This may be the result of surface freshwater inputs, sampled and analyzed on January and April, 2019 (Figure 15), or possible subsurface run-off through the highly permeable sediments.

4.2 Biogeochemistry of the primary channel

4.2.1 Spatial and temporal patterns

The primary channel exhibits biogeochemical conditions that are expected of swashes in the Grand Strand region with overlying water DIN, PO_4^{3-} and Chl *a* concentrations similar to those in discharge waters of Withers Swash (Smith and Sanger 2015). High nutrient concentrations in November, 2018, coincide with very low salinities in the swash (Figure 6) and the coastal ocean (Figure 4), a probable consequence of continued discharge of freshwater accumulated in the upland watersheds during Hurricane Florence.

Sedimentary concentrations of DIN, PO_4^{3-} and Chl *a* are higher than overlying water values on most instances during the study period (Figure 11), consistent with the role of coastal sediments as a major site of organic matter degradation (e.g., Burdige, 2006). The nutrient concentration difference between sediment and overlying water suggests a flux of nutrients towards the SWI. High Sed Chl *a* concentrations are explained by the “benthic nutrient filter” effect, i.e., sediment surface microphytobenthos

intercept sedimentary nutrients before they reach the overlying water (Anderson et al., 2014).

With the exception of sedimentary DIN, sedimentary and overlying water biogeochemical properties vary with the seasons (Figure 9), as predicted by shifts in balance between photosynthesis and respiration driven by light and temperature fluctuations (Figure 4). Based on ongoing time-series monitoring of Long Bay beaches (Hannides et al., in prep.), sandy sediments experience annual minimum Chl *a* concentrations in October-November, a major maximum period in June-August and a minor one (“spring bloom”) in February-March. Accordingly, Chl *a* and O₂ are elevated and nutrient concentrations suppressed in August, 2018, and January, 2019, with the inverse observed in December, 2017, and November, 2018.

4.2.2 Non-conservative behavior

The results of the conservative mixing analysis indicate that monitored properties exhibit non-conservative behavior for most of the study period (Figure 10). Pore-water nutrients exhibit source behavior in all seasons except August (a net balance between source and sink), a finding consistent with a role of sandy sediments as a biofilter, whereby overlying water organic matter is filtered and respired to generate inorganic nutrients (Boudreau et al., 2001).

The fate of the generated inorganic nutrients is seasonally dependent, as this study’s conservative mixing analysis reflects these general patterns (Table 2, Figure 10). We assume that land-derived organic matter is filtered by the sandy terminus of the swash, and is respired by sedimentary microbiota. Turbulent mixing will transport these

nutrients to the sediment surface where they are intercepted by the benthic nutrient filter. We also assume that any land-derived dissolved nutrients in overlying water will also be taken up primarily by benthic photosynthesizers since Sed Chl *a* is much more concentrated than overlying-water Chl *a* (Figure 11). The swash is a source for O₂ and both overlying and Sed Chl *a* during the peak- Chl *a* period in this region (August), while in the low- Chl *a* period (November/December) it is a sink for Chl *a* and a source for nutrients. By January, source-sink behavior already reverts to conditions representative of higher Chl *a*, i.e., primary productivity.

4.3 Human activities and their effects

4.3.1 Run-off from the surrounding area

The patterns described in the previous section can be explained by well-established understanding of seasonal variations and the interaction between overlying water and highly permeable sediment. The data from April, 2019, however, are inconsistent with this pattern. Overlying water is undersaturated with respect to O₂ and high in nutrients, compared to January, 2019. However, conservative mixing analysis indicates a sink for O₂, overlying water DIN and Sed Chl *a* and a source for overlying water PO₄³⁻ (4/14/2019, Figure 7 and Figure 8).

An explanation for this exception is input of freshwater from surface run-off flowing into the middle of the primary channel transect from adjacent lawns at relatively high rates. We observed, sampled and analyzed surface run-off in both January and April, 2019, and we note, by observation, that both flow rate and occurrence of point flows were

much higher in April and it coincided with substantial macroalgal overgrowth on hard substrate on the banks of the primary channel (Figure 14). Respiration of this overgrowth would result in O₂ draw-down and the occurrence of denitrification that would selectively remove nitrate but not PO₄³⁻ from the system, thus explaining both the patterns in overall concentrations and sink-source behavior.

Seasonal changes in human practices, especially daily irrigation and fertilizer application, may exacerbate nutrient loading to the coastal zone and stimulate eutrophic conditions characterized by excess primary production and O₂ draw-down (Sanger et al., 2012; Troup et al., 2017).

4.3.2 Channel management

Channel realignment is a regular practice at Singleton Swash (USACE and DHEC, 2014). One such realignment took place during our study in December, 2018. The result was a reduction of the total length of the primary channel by approximately 30 %. While we sampled on a well-defined spatial transect before (November) and after (January), seasonally-driven natural and anthropogenic process changes over this period prevent us from demonstrating the immediate impacts of this realignment. In principle, the shortening of the distance over which overlying water solutes can interact with the underlying highly permeable sand and be modified may result in higher concentrations of nutrients at the ocean-most stations of our transect. A follow-up study during which the swash is monitored shortly before and after realignment should test for the impacts of the manipulation of the primary channel length on nutrient discharges to the coastal ocean.

Construction of a concrete culvert would change one critical aspect of the primary channel: the surface area of the underlying substrate. Sediment provides a much higher surface area per unit volume (or per meter-distance of a channel) than an impervious surface. Biofilms (and perhaps macroalgal mats) will inevitably form on the impervious surface and transform matter as it passes over them. Given our findings that show significant reservoirs of nutrients in sand, in the case of absence of the sandy substrate, those nutrients would otherwise have to be stored in hard-substrate epibiota or be exported to either side of the impervious culvert. Consideration must be given to the design of such a culvert and its potential impacts on the exchange of dissolved constituents between marsh and coastal ocean.

5 CONCLUSIONS

This transect study of the shoreline segment of Singleton Swash documents a highly permeable primary channel whose biogeochemistry responds with the seasons, with evidence of low primary productivity in November-December and higher primary productivity in August. Conservative mixing analysis indicates that the channel's sandy sediments act as a biofilter, respiring organic matter and generating inorganic nutrients that, outside the low primary productivity period, are exploited by benthic photosynthesizers.

Detection of a gradual freshwater-seawater transition along the transect was complicated by freshwater inputs as surface run-off from surrounding properties in January and April, 2019. These inputs were substantial on the latter date and high in nutrients and are the most likely reason for macroalgal overgrowth on hard substrate. Replacement of the sandy bottom of the channel with an impervious culvert may require epibiota such as macroalgae to remove excess nutrients, otherwise these nutrients will be exported to the coastal ocean or the marsh. The presence of a highly permeable sand column may currently be serving as an effective remediation strategy for these inputs and deserves further study.

6 REFERENCES

- Allen, J. R. (1968). Current ripples: Their relation to patterns of water and sediment motion. Amsterdam: North-Holland.
- Anderson, I.C., Brush, M.J., Piehler, M.F., Currin C.A., Stanhope, J.W., Smyth, A.R., Maxey, J.D., and Whitehead, M.L. (2014). Impacts of Climate-Related Drivers on the Benthic Nutrient Filter in a Shallow Photic Estuary. *Estuaries and Coasts*, 37 (Suppl 1): S46–S62.
- Arar, E.J., and Collins G.B. (1997) Method 445.0 – In vitro determination of chlorophyll a and pheophytin a in marine and freshwater algae by fluorescence. U.S. EPA.
- Arnold, C. L., and Gibbons, C. J. (1996). Impervious Surface Coverage: The Emergence of a Key Environmental Indicator. *Journal of the American Planning Association*, 62(2), 243-258.
- Barnhardt, W.A. (2009). Coastal change along the shore of northeastern South Carolina—The South Carolina coastal erosion study: U.S. Geological Survey Circular 1339, 77 p.
- Bendschneider, K. and Robinson, R. J. (1952). A new spectrophotometric method for the determination of nitrite in seawater. *Journal of Marine Research*, 11: 87-96.
- Berg, P., Røy, H., Janssen, F., Meyer, V., Jørgensen, B., Huettel, M., and Beer, D. D. (2003). Oxygen uptake by aquatic sediments measured with a novel non-invasive eddy-correlation technique. *Marine Ecology Progress Series*, 261, 75-83.
- Berner, R. A. (1980). Early diagenesis: a theoretical approach (No. 1). Princeton University Press.

- Berner, E. K., and Berner, R. A. (1987). The global water cycle: Geochemistry and environment. Englewood Cliffs, NJ: Prentice-Hall.
- Boudreau, B. P., M. Huettel, S. Forster, R. A. Jahnke, A. McLachlan, J. J. Middelburg, P. Nielsen, F. J. Sansone, G. L. Taghon, W. Van Raaphorst, I. T. Webster, J. M. Weslawski, P. Wiberg and B. Sundby (2001) Permeable marine sediments: overturning an old paradigm. *Eos, Transactions of the American Geophysical Union*, 82: 133, 135-136.
- Boulton, A. J., Findlay, S., Marmonier, P., Stanley, E. H., and Valett, H. M. (1998). The functional significance of the hyporheic zone in streams and rivers. *Annual Review of Ecology and Systematics*, 29(1), 59-81.
- Burdige, D. J. (2006) Geochemistry of marine sediments. Princeton University Press, Princeton, New Jersey, U.S.A., pp. 609.
- Chipman, L., Berg, P., and Huettel, M. (2016). Benthic Oxygen Fluxes Measured by Eddy Covariance in Permeable Gulf of Mexico Shallow-Water Sands. *Aquatic Geochemistry*, 22(5-6), 529-554.
- Elliot, A. H., and Brooks, N. H. (1997). Transfer of nonsorbing solutes to a streambed with bed forms: Laboratory experiments. *Water Resour. Res*, 33(1), 137-151.
- Froelich, P., Klinkhammer, G., Bender, M., Luedtke, N., Heath, G., Cullen, D., Maynard, V. (1979). Early oxidation of organic matter in pelagic sediments of the eastern equatorial Atlantic: Suboxic diagenesis. *Geochimica Et Cosmochimica Acta*, 43(7), 1075-1090.

- Hannides, A.K., Glazer, B.T., and Sansone, F.J., (2014). Extraction and quantification of microphytobenthic Chl a within calcareous reef sands. *Limnology and Oceanography*, 12: 126-138.
- Hansen, H. P., and Koroleff, F. (1999). Determination of nutrients. *Methods of Seawater Analysis*, 159-228.
- Hedges, J. I., and Keil, R. G. (1995). Sedimentary organic matter preservation: an assessment and speculative synthesis. *Marine chemistry*, 49(2-3), 81-115.
- Hoffnagle, B. L. (2015). Linking water quality and beach morphodynamics in a heavily impacted tidal creek in Myrtle Beach, South Carolina. *Electronic Theses and Dissertations*. 23.
- Holland, A., Sanger, D. M., Gawle, C. P., Lerberg, S. B., Santiago, M. S., Riekerk, G. H., . . . Scott, G. I. (2004). Linkages between tidal creek ecosystems and the landscape and demographic attributes of their watersheds. *Journal of Experimental Marine Biology and Ecology*, 298(2), 151-178.
- Holmes, R.M., Aminot, A., K  rouel, R., Hooker, B.A., and Peterson, B.J. (1999). A simple and precise method for measuring ammonium in marine and freshwater ecosystems. *Canadian Journal of Fisheries and Aquatic Sciences*, 56 1801-1808.
- Howarth, R., Chan, F., Conley, D. J., Garnier, J., Doney, S. C., Marino, R., and Billen, G. (2011). Coupled biogeochemical cycles: Eutrophication and hypoxia in temperate estuaries and coastal marine ecosystems. *Frontiers in Ecology and the Environment*, 9(1), 18-26.

- Huettel, M., Berg, P. and Kostka, J. (2014). Benthic Exchange and Biogeochemical Cycling in Permeable Sediments. *Annual Review of Marine Science*, 6(1), pp.23-51.
- Huettel, M., and Gust, G. (1992). Impact of bioturbation on interfacial solute exchange in permeable sediments. *Marine Ecology Progress Series*, 89, 253-267.
- Huettel, M., Ziebis, W., and Forster, S. (1996). Flow-induced uptake of particulate matter in permeable sediments. *Limnology and Oceanography*, 41(2), 309-322.
- Huettel, M., Ziebis, W., Forster, S., and Luther III, G. W. (1998). Advective transport affecting metal and nutrient distributions and interfacial fluxes in permeable sediments. *Geochimica et Cosmochimica Acta*, 62(4), 613-631.
- Hjulstrom, F. (1939). Transportation of detritus by moving water: Part 1. Transportation. In P. D. Trask (Ed.), *Recent marine sediments. A Symposium: Tulsa, Oklahoma* (pp. 5–31). Tulsa, OK: AAPG.
- Kim, K. H., Heiss, J. W., Michael, H. A., Cai, W. J., Laattoe, T., Post, V. E., and Ullman, W. J. (2017). Spatial patterns of groundwater biogeochemical reactivity in an intertidal beach aquifer. *Journal of Geophysical Research: Biogeosciences*, 122(10), 2548-2562.
- Klute, A., and Dirksen, C. (1986). Hydraulic conductivity and diffusivity: laboratory methods, In A. Klute [ed.], *Methods of soil analysis, Part 1: Physical and mineralogical methods*. American Society of Agronomy—Soil Science Society of America, 687-734.
- Libes, S. (2011). *Introduction to marine biogeochemistry*. Academic Press.

- LBOS (2019). Apache Pier data record on SECOORA, retrieved from SECOORA Data Portal, accessed at <https://portal.secoora.org>.
- MacIntyre, H. L., Geider, R. J., and Miller, D. C. (1996). Microphytobenthos: the ecological role of the “secret garden” of unvegetated, shallow-water marine habitats. I. Distribution, abundance and primary production. *Estuaries*, 19(2), 186-201.
- McManus, J., (1988). Grain size determination and interpretation. In Tucker, M. E. (ed.), *Techniques in Sedimentology*. Oxford: Blackwell Scientific, pp. 63–85.
- Murphy, J. and Riley, J. P., (1962) A modified single solution method for the determination of phosphate in natural waters. *Analytica Chimica Acta*, 27: 31-36.
- National Ocean Service, NOAA. (2013). National Coastal Population Report: Population Trends from 1970 to 2020 NOAA’s State of the Coast (Report).
- National Weather Service (2019). Preliminary Monthly Climate Data (CF6), North Myrtle Beach (Wilmington, NC, Forecast Office), retrieved from <https://w2.weather.gov/climate/index.php?wfo=ilm>.
- Pastore, D., (2018). Hydrodynamic Drivers of Dissolved Oxygen Variability Within a Highly Developed Tidal Creek in Myrtle Beach, South Carolina. *Electronic Theses and Dissertations*. 40.
- Peterson, R. N., Moore, W. S., Chappel, S. L., Viso, R. F., Libes, S. M., and Peterson, L. E. (2016). A new perspective on coastal hypoxia: The role of saline groundwater. *Marine Chemistry*, 179, 1-11.

- Pinckney, J., Paerl, H. W., and Fitzpatrick, M. (1995). Impacts of seasonality and nutrients on microbial mat community structure and function. *Marine Ecology Progress Series*, 123, 207-216.
- Precht, E., and Huettel, M. (2004). Rapid wave-driven advective pore water exchange in a permeable coastal sediment. *Journal of Sea Research*, 51(2), 93-107.
- Raymond, P. A., Bauer, J. E., and Cole, J. J. (2000). Atmospheric CO₂ evasion, dissolved inorganic carbon production, and net heterotrophy in the York River estuary. *Limnology and Oceanography*, 45(8), 1707-1717.
- Rocha, C., Forster, S., Koning, E., and Epping, E. (2005). High-resolution permeability determination and two-dimensional porewater flow in sandy sediment. *Limnology and Oceanography: Methods*, 3(1), 10-23.
- Sanger, D., Smith, E., Voulgaris, G., Koepfler, E., Libes, S., Riekerk, G., . . . Whitaker, J. (2012). Constrained enrichment contributes to hypoxia formation in Long Bay, South Carolina (USA), an open water urbanized coastline. *Marine Ecology Progress Series*, 461, 15-30.
- Savant, S. A., Reible, D. D., and Thibodeaux, L. J. (1987). Convective transport within stable river sediments. *Water Resources Research*, 23(9), 1763-1768.
- Schutte, C., Hunter, K., McKay, P., Iorio, D. D., Joye, S., and Meile, C. (2013). Patterns and Controls of Nutrient Concentrations in a Southeastern United States Tidal Creek. *Oceanography*, 26(3), 132-139.
- Strickland, J.D.H., and Parsons, T.R. (1972). A practical handbook of sea-water analysis. *Fisheries Research Board Canada Bulletin* 167, 310.

- Smith, E., and Sanger, D. (2015). Determining the Role of Estuarine Swashes on Water Quality Impairment along the Grand Strand of South Carolina: Impacts of Land Use and Stormwater Runoff. National Estuarine Research Reserve System Science Collaborative (Final Report).
- Sokal, R.R., and Rohlf, F.J. (1994). Biometry. 3rd ed. W.H. Freeman.
- Speybroeck, J., Bonte, D., Courtens, W., Gheskiere, T., Grootaert, P., Maelfait, J. P., ... and Van Lancker, V. (2006). Beach nourishment: an ecologically sound coastal defence alternative? A review. *Aquatic Conservation: Marine and Freshwater Ecosystems*, 16(4), 419-435.
- Troup, M. L., Fribance, D. B., Libes, S. M., Gurka, R., and Hackett, E. E. (2017). Physical Conditions of Coastal Hypoxia in the Open Embayment of Long Bay, South Carolina: 2006–2014. *Estuaries and Coasts*, 40(6), 1576-1591.
- United States United States Army Corps of Engineers (USACE) (2009) Singleton Swash Planning Assistance to States (PAS) Study Horry County, South Carolina, USACE, Charleston District.
- United States United States Army Corps of Engineers (USACE) and The South Carolina Department of Health and Environmental Control (SCDHEC) (2014). Joint Public Notice Singleton Swash Stabilization (P/N # 2014-00013-3H). Charleston, SC: Horry County Government.
- United States United States Army Corps of Engineers (USACE) and The South Carolina Department of Health and Environmental Control (SCDHEC) (2018). Joint Public Notice Singleton Swash Stabilization (P/N # 2014-00013-3H). Charleston, SC: Horry County Government.

USNO (2019). Complete Sun and Moon data for one day, accessed at

https://aa.usno.navy.mil/data/docs/RS_OneDay.php.

Webb, J. E., and Theodor, J. (1968). Irrigation of submerged marine sands through wave action. *Nature*, 220(5168), 682-683.